ADVANCES IN ATMOSPHERIC SCIENCES, VOL. 34, JUNE 2017, 727–736

• **Original Paper** •

Statistical Characteristics of Raindrop Size Distribution in the Tibetan Plateau and Southern China

Yahao WU[1,2] and Liping LIU*[1]

[1]*State Key Laboratory of Severe Weather, Chinese Academy of Meteorological Sciences, Beijing 100081, China*
[2]*China Hunan Meteorological Bureau, Changsha 410007, China*

(Received 28 January 2016; revised 16 October 2016; accepted 21 November 2016)

ABSTRACT

The characteristics of raindrop size distribution (DSD) over the Tibetan Plateau and southern China are studied in this paper, using the DSD data from April to August 2014 collected by HSC-PS32 disdrometers in Nagqu and Yangjiang, comprising a total of 9430 and 6366 1-min raindrop spectra, respectively. The raindrop spectra, characteristics of parameter variations with rainfall rate, and the relationships between reflectivity factor (Z) and rainfall rate (R) are analyzed, as well as their DSD changes with precipitation type and rainfall rate. The results show that the average raindrop spectra appear to be one-peak curves, the number concentration for larger drops increase significantly with rainfall rate, and its value over southern China is much higher, especially in convective rain. Standardized Gamma distributions better describe DSD for larger drops, especially for convective rain in southern China. All three Gamma parameters for stratiform precipitation over the Tibetan Plateau are much higher, while its shape parameter (μ) and mass-weighted mean diameter ($D_{\rm m}$), for convective precipitation, are less. In terms of parameter variation with rainfall rate, the normalized intercept parameter ($N_{\rm w}$) over the Tibetan Plateau for stratiform rain increases with rainfall rate, which is opposite to the situation in convective rain. The μ over the Tibetan Plateau for stratiform and convective precipitation types decreases with an increase in rainfall rate, which is opposite to the case for $D_{\rm m}$ variation. In Z–R relationships, like "$Z = AR^b$", the coefficient A over the Tibetan Plateau is smaller, while its b is higher, when the rain type transfers from stratiform to convective ones. Furthermore, with an increase in rainfall rate, parameters A and b over southern China increase gradually, while A over the Tibetan Plateau decreases substantially, which differs from the findings of previous studies. In terms of geographic location and climate over the Tibetan Plateau and southern China, the precipitation in the pre-flood seasons is dominated by strong convective rain, while weak convective rain occurs frequently in northern Tibet with lower humidity and higher altitude.

Key words: Tibetan Plateau, raindrop size distribution, precipitation classification, standardized gamma distribution

Citation: Wu, Y. H., and L. P. Liu, 2017: Statistical characteristics of raindrop size distribution in the Tibetan Plateau and southern China. *Adv. Atmos. Sci.*, **34**(6), 727–736, doi: 10.1007/s00376-016-5235-7.

1. Introduction

As the largest and highest plateau in the world, the average elevation over a large area of the Tibetan Plateau can reach up to the middle troposphere. The dynamic and thermodynamic forcing of the Tibetan Plateau exerts great impacts on atmospheric moisture and energy cycles and related convective activities, which subsequently affect ecological processes in the downstream areas of the Tibetan Plateau (Tao and Ding, 1981; Huang, 1985; Huang and Sun, 1994). Shi et al. (2008a) argued that atmospheric moisture could be transported from the Tibetan Plateau to the Yangtze River Basin via the interaction between the orographic dynamical forcing and the abundant atmospheric moisture over the southern highlands around the Tibetan Plateau. The airflow originated from Tibet is forced to rise due to topographic obstruction and surface heating, triggering the development of convective activities and heavy rainstorms in southern China (He and Li, 2013; Li et al., 2014).

Over the past three decades, much attention has been paid nationwide to observations of raindrop size distribution (DSD). Great progress has been made in this regard, especially in the development of advanced measuring instruments and analytical approaches. Chen and Gu (1989) studied the characteristics of average DSD based on observations of heavy rainfall events in Changchun, Jilin Province. Qing et al. (1994) summarized the DSD characteristics for a vortex-induced cloud system in Chengdu, Sichuan Province. Niu et al. (2002) analyzed DSD parameters associated with various atmospheric circulation patterns and weather systems at seven stations in Ningxia Province. Liu and Lei (2006) summarized some preliminary characteristics of DSD for both stratiform and convective precipitation in the Bei-

* Corresponding author: Liping LIU
Email: lpliu@camscma.cn

jing area, and described the mean diameters, DSD peaks and the relationships between reflectivity factor and rainfall rate (Z–R relationships). Shi et al. (2008a) analyzed the DSD characteristics for convective precipitation, mixed precipitation, and stratiform precipitation around the Qilian Mountains during the summer of 2006. The particle diameters, Z–R relationships, and the distribution of fall velocity were revealed. Zhang et al. (2009) summarized the differences in DSD among three precipitation systems in Menyuan, Qinghai Province, and analyzed their formation mechanisms. Liao et al. (2011) investigated DSD characteristics for a typical typhoon precipitation event and a frontal precipitation event that occurred in the summer in the Pearl River Delta region. Chen et al. (2013b) analyzed the spatio temporal variations of DSD during the mei-yu season over Jianghuai Basin. However, few studies have been conducted to investigate DSD characteristics with respect to the microphysical structure of precipitation over highland areas and their variations with rainfall rate, because of the scarcity of ground observations in such areas. Studies on the differences and similarities of rainfall characteristics between the Tibetan Plateau and southern China have received little attention so far. In terms of geographic location and climate over the Tibetan Plateau and southern China, it is well known that the precipitation in the pre-flood seasons is dominated by strong convective rain, while weak convective rain occurs frequently in northern Tibet with lower humidity and higher altitude. Li and Su (2014) compared conventional observations collected at 10 weather stations over the Tibetan Plateau and southern China and concluded air pollution could suppress light rainfall processes.

DSD observation is a key step for microphysical analysis of cloud and precipitation, which forms the basis for the development of microphysical parameterization schemes in numerical models. However, until the late 1990s, almost all microphysical schemes in numerical models used in China were actually developed abroad. The regional differences in cloud-precipitation characteristics and the specific characteristics of microphysical processes in China have been completely ignored in numerical weather prediction (NWP) studies (Fletcher, 1962; Kong et al., 1990; Guo et al., 2001). Hu et al. (1998) developed a simplified explicit scheme to describe mixed-phase clouds and precipitation processes based on the warm cloud scheme. The Global Assimilation and Prediction System (GRAPES) has been under development by the China Meteorological Administration since 2001 (Chen et al., 2008; Xue et al., 2008). The GRAPES model includes a coupled cloud–precipitation scheme that can simulate precipitation well in the pre-flood season over southern China (Zhang and Liu, 2006). Sun et al. (2008) coupled a complex microphysical scheme developed by CAMS (Chinese Academy of Meteorological Sciences) to simulate the hydrometeor distribution during the life cycle of a heavy rainstorm that occurred in northern China, and then investigated the DSD characteristics of the storm. Based on the above discussion, in order to improve the reliability and accuracy of NWP, it is necessary to incorporate microphysical properties of clouds and precipitation into numerical models.

The second Tibetan Plateau Experiment of Atmospheric Science (TIPEX) was conducted in the late 1990s and obtained valuable observations. Using the observations collected at Tibet (Nagqu) during TIPEX, Ueno et al. (2001) investigated convective activities and cloud structures that were associated with weak and frequent monsoon precipitation. Shimizu et al. (2001) detected a diurnal rainfall cycle on the Tibetan Plateau based on analysis of TRMM (Tropical Rainfall Measuring Mission) satellite information and revealed the mesoscale characteristics of stratiform clouds. Uyeda et al. (2001) analyzed the characteristics of convective clouds measured by X-band Doppler radars. Liu et al. (2002) summarized the diurnal precipitation variation over Tibet before and after monsoon onset and revealed their relationships with thermodynamic variables. However, DSD characteristics were not observed and analyzed in this experiment.

During the period from 1 July to 31 August 2014, the third TIPEX was carried out, in which microphysical variables related to clouds and precipitation were measured by advanced instruments in Nagqu, Tibet. In the same year, the southern China Monsoon Rainfall Experiment, funded by the Research and Development Project of the World Meteorological Organization, was conducted in Yangjiang, Guangdong Province. Measurements of DSD by ground-based disdrometers in Tibet and in Guangdong from April to August 2014 is used in this study. The purpose of the present study is to advance our understanding of DSD characteristics over the Tibetan Plateau and southern China. This knowledge would be useful for the evaluation of microphysical parameterization schemes in numerical models over regions in the future. The paper is organized as follows. A description of the dataset and methods is given in section 2. The classification of precipitation type, the average raindrop size distribution, and the parameters in Gamma distributions and their changes with rainfall rate and Z–R relationships over Tibet and southern China are analyzed in section 3. A summary and discussion are given in sections 4 and 5, respectively.

2. Data and methodology

2.1. *Data processing*

During the period from 24 April to 11 June 2014, DSD characteristics were measured at Yangjiang Meteorological Bureau [(21.84°N, 111.98°E); 90 m above mean sea level (AMSL)] with a particle size and velocity disdrometer called HSC-PS32. The disdrometer was also used to observe DSD characteristics at Nagqu Meteorological Bureau [(31.80°N, 92.12°E); 4508 m AMSL] from 24 June to 31 August in the same year. The HSC-PS32 disdrometer is a Chinese version of the OTT Parsivel disdrometer, which is a kind of ground-based optical disdrometer designed to count and measure the fall velocity and precipitation particle size simultaneously in a 32×32 square. The main specifications of the HSC-PS32 disdrometer are shown in Table 1, and Table 2 gives the interval of each grade in rainfall rate. It should be noted that the raindrop diameter of larger than 5 mm has been excluded,

considering its liquid particle size range and the unidentified overlapping particles in heavy precipitation events.

Table 1. Main specifications of the HSC-PS32 disdrometer.

Parameter type	Component		Setting
Electrical	Power supply		220 VAC or 12 VDC/1A 24 VDC/3A (heating)
Optical	Light source		Infrared emitting diode
	Transmission power		3 mW
	Power measurement		54 cm^2 (18 cm × 3 cm)
	Optical wavelength		650 mm
	Optical frequency		50 kHz
Technical	Particle size range	Liquid	0.2–5 mm
		Solid	0.2–25 mm
	Temporal resolution		60 s
	Particle grades		32 × 32
	Velocity range		0.2–20 m s^{-1}
	Rainfall range		0.001–1200 mm h^{-1}
	Reflectivity range		−9.9 – −99 dB*Z*

Table 2. Interval of each grade in size and fall speed.

Grade	Average speed (m s^{-1})	Average particle size (mm)
1	0.05	0.062
2	0.15	0.187
3	0.25	0.312
4	0.35	0.437
5	0.45	0.562
6	0.55	0.687
7	0.65	0.812
8	0.75	0.937
9	0.85	1.062
10	0.95	1.187
11	1.1	1.375
12	1.3	1.625
13	1.5	1.875
14	1.7	2.125
15	1.9	2.375
16	2.2	2.75
17	2.6	3.25
18	3.0	3.75
19	3.4	4.25
20	3.8	4.75
21	4.4	5.5
22	5.2	6.5
23	6.0	7.5
24	6.8	8.5
25	7.6	9.5
26	8.8	11.0
27	10.4	13.0
28	12.0	15.0
29	13.6	17.0
30	15.2	19.0
31	17.6	21.5
32	20.8	24.5

A total of 9430 and 6366 1-min DSD measurements were collected in Tibet and southern China, respectively. The raindrop number concentration per unit volume at a discrete instant could been calculated based on the disdrometer counts:

$$n(D_i) = \sum_{j=1}^{32} \frac{A_{ij}}{V_j T S} , \tag{1}$$

where A_{ij} is the number of raindrops within the size bin i and velocity bin j; T(s) and S(m^2) are the sampling time and area respectively; D_i (mm) is the raindrop diameter for the size bin I; and V_j (m s^{-1}) is the fall speed for the velocity bin j.

Thus, some integral rain parameters, such as radar reflectivity factor Z (dBZ), rainfall rate R (mm h^{-1}), total number density N_a (m^{-3}), and median volume diameter D_0 (mm) could be derived successively, as below. Rainfall rate has direct ratio relations with the third power of particle diameter and raindrop number, and reflectivity factor is proportional to the sixth power of particle diameter and raindrop number per unit volume. It should be noted that the reflectivity factor in Eq. (2) only applies to the Rayleigh scattering and S-band radars:

$$Z = 10\lg\left(\sum_{i=1}^{32} n(D_i) D_i^6\right) ; \tag{2}$$

$$R = \frac{6\pi}{10^4} \sum_{i=1}^{32} \sum_{j=1}^{32} n(D_i) D_i^3 V_j ; \tag{3}$$

$$N_a = \sum_{i=1}^{32} n(D_i) ; \tag{4}$$

$$\sum_{i=0}^{D_{max}} n(D_i) D_i^3 = 2 \sum_{i=0}^{D_0} n(D_i) D_i^3 . \tag{5}$$

2.2. *Raindrop size distribution*

The exponential distribution was widely assumed in many numerical parameterization schemes in the early days (Lin et al., 1983; Rutledge and Hobbs, 1983). The Gamma distribution, proposed by Ulbrich (1983), Eq. (6), has been proven to be a good description for instantaneous DSDs in many regions and rain types (Chen et al., 1998; Ulbrich and Atlas, 1998), while the exponential distribution is an exception of the Gamma distribution when $\mu = 0$:

$$N(D) = N_0 D^{\mu} \exp(-\lambda D) , \tag{6}$$

where N (m^{-3} mm^{-1}) is the raindrop number concentration referring to the raindrop diameter D (mm). The Gamma distribution can be represented by an intercept parameter N_0 (m^{-3} $mm^{-\mu-1}$), a shape parameter μ, and a slope parameter λ (m m^{-1}). However, these three parameters in a Gamma distribution are not mutually independent, and thus the standardized Gamma distribution is used to fit the DSD data, which is given by

$$N(D) = N_w f(\mu) \left(\frac{D}{D_m}\right)^{\mu} \exp\left[-(\mu+4)\frac{D}{D_m}\right] , \tag{7}$$

where N_w (m^{-3} mm^{-1}) is a normalized intercept parameter, indicating the number concentration with exponential distributions that has the same median volume diameter and liquid water content (Liu et al., 2007), and the parameters D_m (mm) and μ are the mass-weighted mean diameter and the shape parameter, respectively.

Moment methods have been widely used to estimate raindrop spectrum parameters for cloud and precipitation in numerical models (Smith, 2003). The *i*th-order moment of DSD is given by Eq. (8). The three independent parameters N_w, μ and D_m could be calculated by the third, fourth and sixth moments of the DSD data described by Kozu and Nakamura (1991), and the parameters $\Gamma(x)$, $f(\mu)$ and G are intermediate ones:

$$M_i = \sum_{i=1}^{32} n(D_i) D^i \ ; \tag{8}$$

$$N_w = \frac{256}{6} \times \frac{M_3^5}{M_4^4} \ ; \tag{9}$$

$$D_m = \frac{M_4}{M_3} \ ; \tag{10}$$

$$G = \frac{M_4^3}{M_3^2 M_6} \ ; \tag{11}$$

$$\mu = \frac{11G - 8 + \sqrt{G(G+8)}}{2(1-G)} \ ; \tag{12}$$

$$\Gamma(x) = \sqrt{2\pi} e^{-x} x^{x-\frac{1}{2}} \ ; \tag{13}$$

$$f(\mu) = \frac{6}{256} \times \frac{(\mu+4)^{\mu+4}}{\Gamma(\mu+4)} \ . \tag{14}$$

3. Results

3.1. *DSD classification of precipitation types*

The case study analysis casts light on some characteristics of the DSD for liquid precipitation regimes occurring over the Tibetan Plateau and southern China during 2014. The behavior of DSD is investigated using the 1-min DSD for selected precipitation types and rain rate intervals. A simple scheme is used to separate stratiform and convective precipitation types based on the standard deviation (σ_R) of the rainfall rate (R) over five consecutive 2-min DSD samples (Bringi et al., 2003), based on $R \geqslant 0.5$ mm h^{-1} and $\sigma_R \leqslant 1.5$ mm h^{-1} for stratiform precipitation, and $R \geqslant 5$ mm h^{-1} and $\sigma_R > 1.5$ mm h^{-1} for convective precipitation. Chen et al. (2013b) also adopted a similar concept to study DSD statistical characteristics in the mei-yu season over eastern China. The rain rate intervals are classified as follows (in mm h^{-1}): $0.1 \leqslant R < 1$ (class 1); $1 \leqslant R < 2$ (class 2); $2 \leqslant R < 5$ (class 3); $5 \leqslant R < 10$ (class 4); $10 \leqslant R < 20$ (class 5); and $R \geqslant 20$ (class 6) (Porcùa et al., 2014). Table 3 shows the relative DSD distributions over the Tibetan Plateau and southern China in precipitation types and rain rate intervals. As can be seen, the stratiform precipitation over the Tibetan Plateau and southern China gives priority to class 1, and then generally decreases with an increase in rainfall rate, especially in the Tibetan Plateau, and there are no distributions of rainfall rate above 10 mm h^{-1}. For convective rain, with an increase in rainfall rate, the DSD distributions over southern China firstly decrease and then increase.

3.2. *Average DSD*

The average DSD for stratiform and convective rain over the Tibetan Plateau and southern China, obtained by averaging all the 1-min DSD data, is shown in Fig. 1. As can be seen, the average raindrop spectra appear to be one-peak curves; and, for stratiform precipitation (Fig. 1a), with an increase in diameter the raindrop number concentration in the Tibetan Plateau has a bigger decrease. Meanwhile, for convective precipitation (Fig. 1b), the raindrop number concentration over southern China is much higher than that over the Tibetan Plateau, with various diameters. The fluctuation of total raindrop number concentration is much more frequent in stratiform precipitation.

Figure 2 shows the changes with average raindrop spectra and rainfall rate for stratiform and convective precipitation over the Tibetan Plateau and southern China. As can be seen, the number concentration for larger drops decreases much less in convective precipitation, especially over the Tibetan Plateau.

3.3. *Discussion on raindrop spectra*

The exponential distribution and the standardized Gamma distribution are chosen to produce a better model for the rain-

Table 3. DSD distributions over the Tibetan Plateau and southern China in rain types and rain rate intervals. The rain types are stratiform and convective precipitation, and the rain rate intervals are (in mm h^{-1}): $0.1 \leqslant R < 1$ (class 1); $1 \leqslant R < 2$ (class 2); $2 \leqslant R < 5$ (class 3); $5 \leqslant R < 10$ (class 4); $10 \leqslant R < 20$ (class 5); and $R \geqslant 20$ (class 6).

	Stratiform precipitation		Convective precipitation	
Rain rate interval	Tibetan Plateau (min)	Southern China (min)	Tibetan Plateau (min)	Southern China (min)
Class 1	1133	404	—	—
Class 2	1249	223	—	—
Class 3	1267	146	—	—
Class 4	124	13	183	27
Class 5	—	—	101	21
Class 6	—	—	52	26

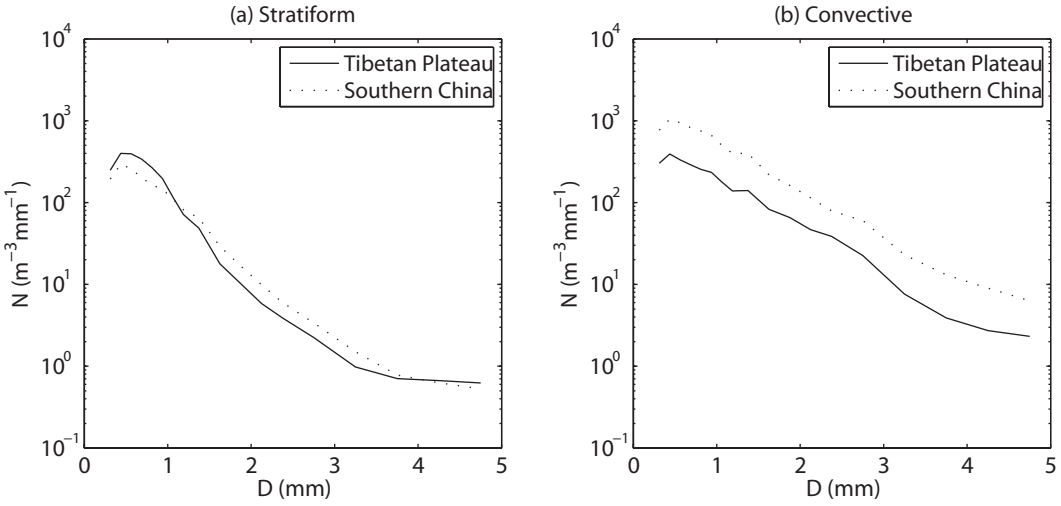

Fig. 1. Average raindrop spectra for (a) stratiform and (b) convective precipitation over the Tibetan Plateau and southern China, based on all the 1-min DSD data. The parameters N (m^{-3} mm^{-1}) and D (mm) are the raindrop number concentration and raindrop diameter, respectively.

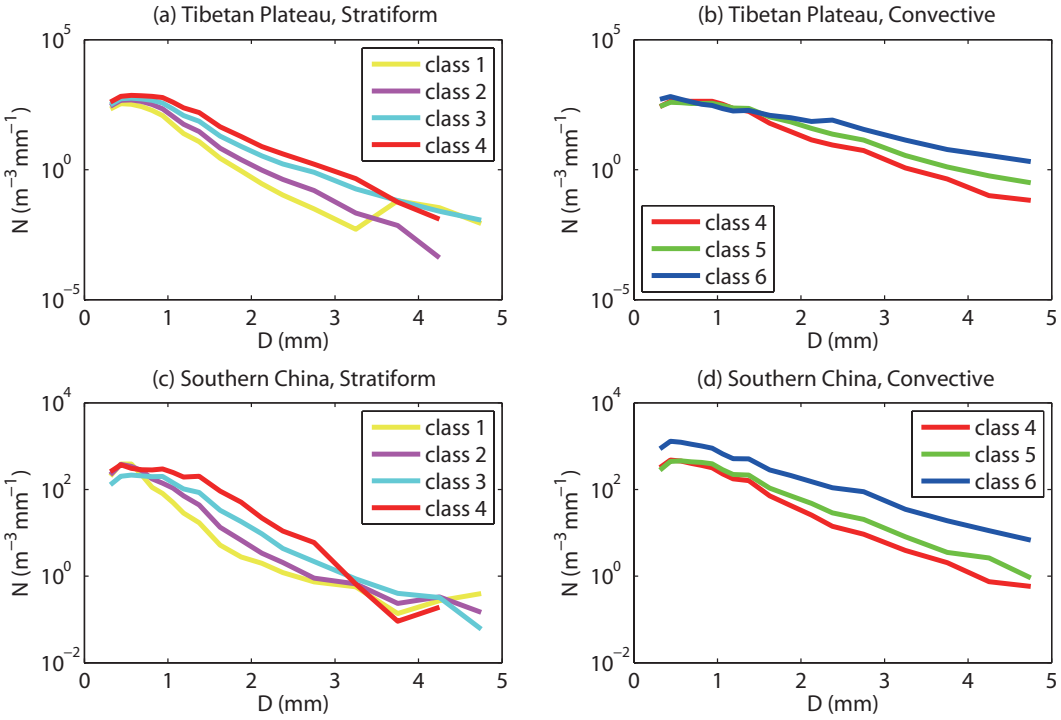

Fig. 2. Average raindrop spectra with rainfall rate for (a, c) stratiform and (b, d) convective precipitation over (a, b) the Tibetan Plateau and (c, d) southern China, based on all the 1-min raindrop data. The parameters N (m^{-3} mm^{-1}) and D (mm) are the raindrop number concentration and raindrop diameter, respectively. The rainfall rate intervals are (in mm h^{-1}): $0.1 \leqslant R < 1$ (class 1); $1 \leqslant R < 2$ (class 2); $2 \leqslant R < 5$ (class 3); $5 \leqslant R < 10$ (class 4); $10 \leqslant R < 20$ (class 5); and $R \geqslant 20$ (class 6).

drop size distribution, based on the moment methods provided in section 2.2. Relative error (RE) between the fitted raindrop number concentration (NC) and the raw raindrop number concentration (NR) is used for evaluation:

$$\mathrm{RE} = \frac{|\mathrm{NC} - \mathrm{NR}|}{\mathrm{NR}} \times 100\%. \qquad (15)$$

Relationships between the REs fitted by samples and the raindrop diameter for precipitation types over the Tibetan Plateau and southern China are shown in Fig. 3. It is noted that the standardized Gamma distribution can better describe the real raindrop spectra, especially for larger drops. For the same area, the fitted RE in convective precipitation is smaller; whereas, in the same rain type, the fitted RE over southern

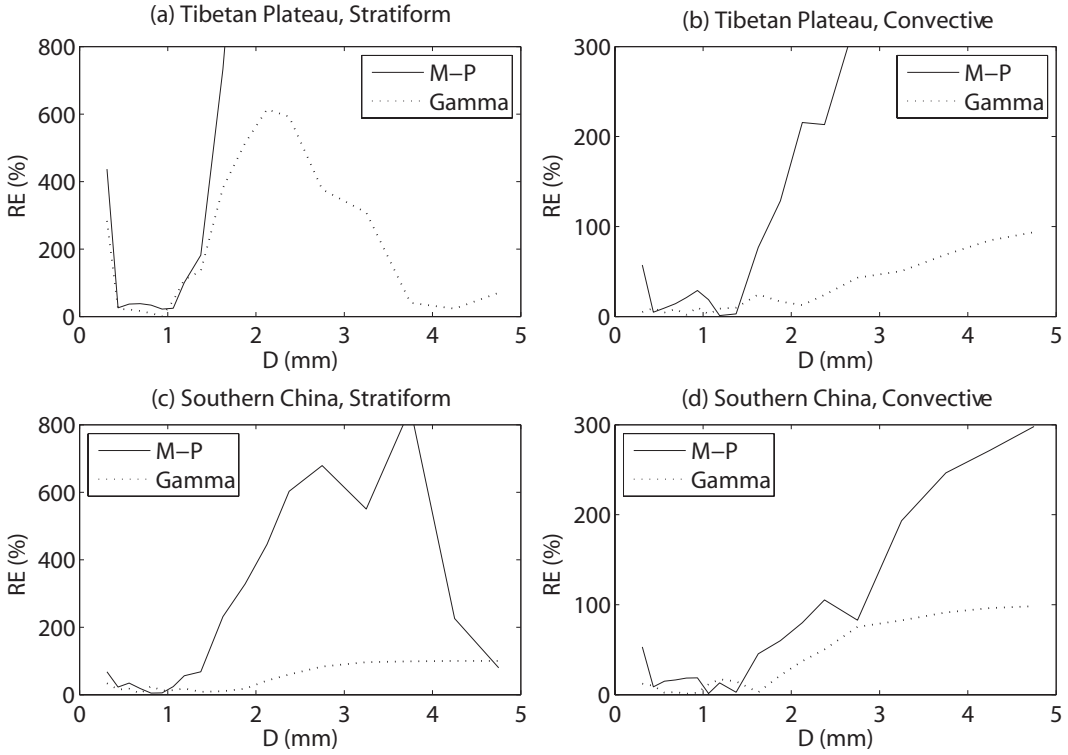

Fig. 3. Plots of relative error (RE, %) fitted by DSD samples and diameter (D, mm) for (a, c) stratiform and (b, d) convective rain over (a, b) the Tibetan Plateau and (c, d) southern China. "M-P" and "Gamma" stand for the exponential distributions and the standardized Gamma distributions, respectively.

China is smaller.

3.4. *Parameters in the Gamma distribution and their changes with rainfall rate*

As three independent parameters in the standard Gamma distribution, the normalized intercept parameter N_w (m^{-3} mm^{-1}), the shape parameter μ, and the mass-weighted mean diameter D_m (mm) can successfully represent the raindrop density, average diameter, and many other spectral characteristics. Table 4 gives the average values of parameters in the standardized Gamma distribution, indicating that all three independent parameters (N_w, μ and D_m), for stratiform rain over the Tibetan Plateau, are larger than those over southern China, especially N_w. Meanwhile, for convective precipitation, the N_w and μ in the Tibetan Plateau are less than those over southern China. Comparing the precipitation in the same area, the N_w and μ for stratiform rain are larger than those for convective rain, while its D_m is less; and the N_w and μ are much higher for stratiform precipitation than those for convective rain, while its D_m is less.

In order to study the relationships between raindrop spectral parameters and rainfall rate, the average value of N_w, μ and D_m in six rain rate intervals over the Tibetan Plateau and southern China, for stratiform and convective precipitation, are shown in Table 5. It is shown that the N_w and D_m for stratiform precipitation over the Tibetan Plateau increases with rainfall rate, but the μ does an opposite trend; and the N_w for stratiform precipitation over southern China decreases with rainfall rate, with its μ decreasing firstly and then increasing with increased rainfall rate, and its D_m increasing. Meanwhile, for the same rainfall rate, the three Gamma parameters for stratiform rain over the Tibetan Plateau are much higher. The N_w and μ for convective precipitation over the Tibetan Plateau decrease with rainfall rate, and the D_m would increase with rainfall rate. The N_w and μ for convective precipitation over southern China increases firstly and then decreases with increased rainfall rate, but the D_m decreases firstly and then increases with the increased rainfall rate. Meanwhile, for the same rainfall rate, the μ over Tibet for convective precipitation is smaller, while the D_m over the Tibetan Plateau for convective precipitation is higher.

3.5. *Z–R relationships*

The power-law relationship between reflectivity factor and rainfall rate, like $Z = AR^b$, is a longstanding problem in quantitative precipitation forecasting, and is strongly affected by altitude differences (Uijlenhoet, 2001). The coefficients A and b are closely related to the raindrop size distribution, particle diameter, radar signal attenuation, and so on (Rosenfeld and Ulbrich, 2003; Chandrasekar et al., 2003). High A values and low b values describe convective midlatitude precipitation, while the opposite is true for tropical precipitation (Tokay and Short, 1996; Caracciolo et al., 2006). Choosing the appropriate A and b based on precipitation types could improve regional rainfall estimation (Shi et al., 2004). The relationship $Z = 300R^{1.4}$ for convective rain,

Table 4. Average values of standardized Gamma distribution parameters for the stratiform rain and convective rain over the Tibetan Plateau and southern China. The N_w (m^{-3} mm^{-1}), μ and D_m (mm) are the normalized intercept parameter, shape parameter, and mass-weighted mean diameter, respectively.

	Stratiform precipitation		Convective precipitation	
Parameter	Tibetan Plateau	Southern China	Tibetan Plateau	Southern China
N_w (m^{-3} mm^{-1})	7243.51	1473.26	5374.12	6345.17
μ	8.58	6.76	7.38	17.66
D_m (mm)	1.07	0.43	1.82	1.48

Table 5. Average values of standardized Gamma distribution parameters for rain types and rain rate intervals over the Tibetan Plateau and southern China. The N_w (m^{-3} mm^{-1}), μ and D_m (mm) are the normalized intercept parameter, shape parameter, and mass-weighted mean diameter, respectively. Rain types are stratiform and convective ones. Rain rate intervals are (in mm h^{-1}): $0.1 \leqslant R < 1$ (class 1); $1 \leqslant R < 2$ (class 2); $2 \leqslant R < 5$ (class 3); $5 \leqslant R < 10$ (class 4); $10 \leqslant R < 20$ (class 5); and $R \geqslant 20$ (class 6).

		Stratiform precipitation		Convective precipitation	
Parameter	Rain rate interval	Tibetan Plateau	Southern China	Tibetan Plateau	Southern China
N_w (m^{-3} mm^{-1})	Class 1	5758.06	1598.53	—	—
	Class 2	7600.98	1581.55	—	—
	Class 3	7692.84	1036.86	—	—
	Class 4	9838.86	623.63	6674.16	6666.00
	Class 5	—	—	4587.01	7005.45
	Class 6	—	—	2385.26	5483.28
μ	Class 1	11.31	10.05	—	—
	Class 2	9.04	3.33	—	—
	Class 3	5.97	3.39	—	—
	Class 4	5.51	1.54	7.83	14.34
	Class 5	—	—	7.18	23.07
	Class 6	—	—	6.20	16.80
D_m (mm)	Class 1	0.95	0.35	—	—
	Class 2	1.03	0.40	—	—
	Class 3	1.20	0.65	—	—
	Class 4	1.31	0.73	1.58	1.55
	Class 5	—	—	1.92	1.43
	Class 6	—	—	2.48	1.45

proposed by Fulton et al. (1998), has been widely used in NEXRAD (Next-Generation Weather Radar), while the relationship $Z = 200R^{1.6}$ is commonly applied to midlatitude areas for stratiform rain (Marshall and Palmer, 1948). However, whilst studies on Z–R relationships in China have been conducted since the early 1990s (Xu et al., 1990; Xu, 1992; Liu et al., 2008), the relationships in Tibet have rarely been involved, let alone any comparisons made among regions. Scatter plots of Z–R relationships and fitted power-law relationships based on least-squares methods for rain types over the Tibetan Plateau and southern China are shown in Fig. 4. The results indicate that the coefficient A over the Tibetan Plateau is smaller than that over southern China, while its value of b is higher, especially for convective precipitation. When the rain type transfers from stratiform rain to convective rain, the coefficient A over the Tibetan Plateau decreases with rainfall rate, while its b increases. Meanwhile, the A and b over southern China increase with rainfall rate, which is different from the findings of previous studies (Hagen and Yuter, 2003). Comparing the results in similar areas, Tokay and Short (1996) found that ($A = 367$, $b = 1.30$) for stratiform cases and ($A = 139$, $b = 1.43$) for convective cases could describe tropical precipitation well; Zhao et al. (2011) found markedly different values for A and b in the Heihe river basin (1500 m AMSL, in the northeastern part of the Tibetan Plateau), reporting ($A = 378$, $b = 1.72$) for stratiform rain and ($A = 244$, $b = 1.79$) for convective rain; Federico Porcùa et al. (2014) carried out disdrometric campaigns in Lhasa (3600 m AMSL), Linzhi (3300 m AMSL) and Namco (4700 m AMSL) in the central-eastern part of the Tibetan Plateau, and reported results of $A = 247$ ($A = 214$) and $b = 1.15$ ($b = 1.25$) for stratiform (convective) precipitation. Possible reasons for such different values could be linked to the altitude/air density, physical properties, data quality control, data fitting, and so on (Cifelli et al., 2000).

4. Summary

A comparison of raindrop characteristics between the Tibetan Plateau and southern China is discussed in this paper, using a total of 9430 and 6366 1-min raindrop spectra samples, respectively, which were collected by HSC-PS32 dis-

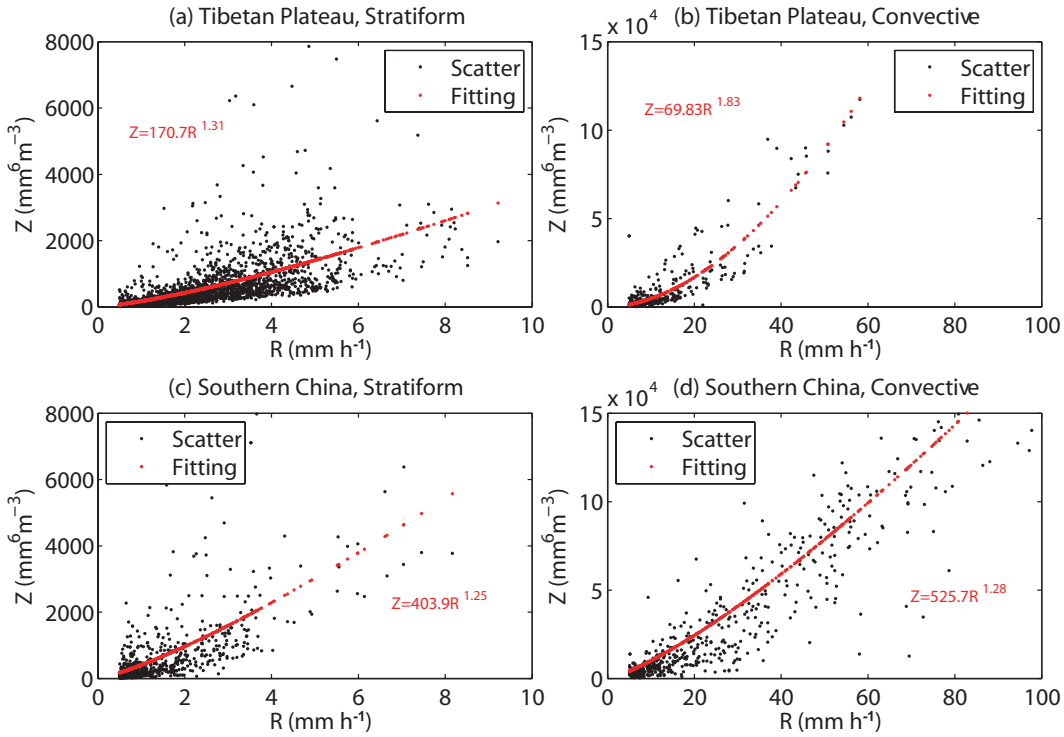

Fig. 4. Scatter plots of radar reflectivity factor and rainfall rate for (a, c) stratiform and (b, d) convective precipitation over (a, b) the Tibetan Plateau and (c, d) southern China. The fitted power-law relationships, $Z = AR^b$, derived from the least-squares method, are also provided.

drometers from April to August 2014. The data are divided into stratiform precipitation and convective precipitation, and the rainfall rate in each rain type is classified into six classes. The main conclusions can be summarized as follows:

(1) The major rainfall rate interval for stratiform rain over the Tibetan Plateau and southern China is class 1, and then generally decreases with an increase in rainfall rate, especially in the Tibetan Plateau, and there are no distributions of rainfall rate above 10 mm h^{-1}. Additionally, the DSD distributions over southern China firstly decrease, and then increase, with an increase in rainfall rate.

(2) The average raindrop spectra seem to be one-peak curves. The raindrop number concentration for stratiform rain over the Tibetan Plateau has a bigger decrease with increased diameter. In convective precipitation, the raindrop number concentration over southern China is much higher than that over the Tibetan Plateau, with various diameters. Furthermore, the number concentration for larger drops has a much more significant increase with rainfall rate, especially in convective rain.

(3) The standardized Gamma distribution better describes real raindrop spectra, especially for larger drops. Compared with the precipitation in the same area, the fitted RE for convective rain is smaller; whereas, for the same rain type, the fitted RE over southern China is smaller.

(4) The three independent parameters for stratiform precipitation over the Tibetan Plateau are larger than over southern China, especially for N_w. Meanwhile, in convective precipitation, the N_w and μ in the Tibetan Plateau are less. The N_w and μ for stratiform rain are larger than those for convective rain, while its D_m is less; the N_w and μ are much higher for stratiform rain than those for convective rain, while its D_m is less.

(5) Referring to the standardized Gamma distribution parameter variation with rainfall rate, the mass-weighted diameter generally increases with rainfall rate, the normalized intercept parameter increases firstly and then decreases, and the shape parameter is inversely proportional to rainfall rate, whose parameter oscillation over southern China is much more frequent than that over the Tibetan Plateau. Meanwhile, the mass-weighted diameter and the shape parameter over the Tibetan Plateau for stratiform precipitation are less than those over southern China.

(6) In Z–R relationships, the coefficient A over the Tibetan Plateau is smaller, while b is higher. When the precipitation type transfers from stratiform to convective, the coefficients A and b over southern China increase gradually with an increase in rainfall rate, while the A over the Tibetan Plateau decreases.

5. Discussion

Since convective precipitation over the Tibetan Plateau features small horizontal scales, short duration, and rapid change (Zhuang et al., 2013), the raindrop number concentration for convective ones over the Tibetan Plateau is less than that over southern China, while its shape parameter and particle diameter is larger, indicating the number of raindrops

per unit volume is less and the raindrop concentration of larger particles decreases rapidly. The more raindrop splits over southern China for convective precipitation is one of the reasons, however, there would be much more evaporation in the Tibetan Plateau for its lower humidity (Niu et al., 2002). In Z–R relationships ($Z = AR^b$), the coefficients change with geographical location, weather conditions, and so on; However, referring to the discussed Z–R relationships, there are some considerable differences with previous studies, a subtle discrepancy in quality control, data fitting, raindrop physical properties are the possible reasons, such as, small raindrops tends to yield the smaller coefficients.

Acknowledgements. The first author thanks Mr. Liping LIU at the State Key Laboratory of Severe Weather, Chinese Academy of Meteorological Sciences, for his guidance. The authors thank Dr. Ming CHEN at the Earth Science Service for Consulting and polishing the manuscript. We also thank the State Key Laboratory of Severe Weather for the assistance in collecting the disdrometer data. The study was supported jointly by the China Meteorological Administration Special Public Welfare Research Fund (Grant No. GYHY201406001), the National (Key) Basic Research and Development (973) Program of China (Grant No. 2012CB417202), and the National Natural Science Foundation of China (Grant No. 41175038).

REFERENCES

Bringi, V. N., V. Chandrasekar, and J. Hubbert, 2003: Raindrop size distribution in different climatic regimes from disdrometer and dual-polarized radar analysis. *J. Atmos. Sci.*, **60**, 354–365.

Caracciolo, C., F. Prodi, A. Battaglia, and F. Porcu, 2006: Analysis of the moments and parameters of a gamma DSD to infer precipitation properties: A convective stratiform discrimination algorithm. *Atmospheric Research*, **80**, 165–186.

Chandrasekar, V., R. Meneghini, and I. Zawadzki, 2003: Global and local precipitation measurements by radar. *Meteor. Monogr.*, **30**, 215.

Chen, B. J., Z. H. Li, J. C. Liu, and F. J. Gong, 1998: Model of raindrop size distribution in three types of precipitation. *Acta Meteorologica Sinica*, **56**, 506–512. (in Chinese with English abstract)

Chen, B. J., J. Yang, and J. P. Pu, 2013a: Statistical characteristics of raindrop size distribution in the Meiyu season observed in eastern China. *J. Meteor. Soc. Japan*, **91**, 215–227.

Chen, D. H., and Coauthors, 2008: New generation of multi-scale NWP system (GRAPES): General scientific design. *Chinese Science Bulletin*, **53**, 3433–3445.

Chen, D. L., and S. F. Gu, 1989: Research on the mean spectrum of the rain storm. *Acta Meteorologica Sinica*, **47**, 124–127. (in Chinese with English abstract)

Chen, L., B. J. Chen, J. Yang, J. P. Pu, H. J. Liu, and Z. H. Gao, 2013b: Characteristics of raindrop size distribution of rainstorm on Meiyu front during 2009–2010. *Transactions of Atmospheric Sciences*, **36**, 481–488. (in Chinese with English abstract)

Cifelli, R., C. R. Williams, D. K. Rajopadhyaya, S. K. Avery, K. S. Gage, and P. T. May, 2000: Drop-size distribution characteristics in tropical mesoscale convective systems. *J. Appl. Meteor.*, **39**, 760–777.

Fletcher, N. H., 1962: *The Physics of Rain Clouds*. Cambridge University Press, 386pp.

Fulton, R. A., J. P. Breidenbach, D.-J. Seo, and D. A. Miller, 1998: The WSR-88D rainfall algorithm. *Wea. Forecasting*, **13**, 377–395.

Guo, X. L., M. Y. Huang, Y. C. Hong, H. Xiao, and L. Zhou, 2001: A study of three-dimensional hail-category hailstorm model part II: Characteristics of hail-category size distribution. *Chinese Journal of Atmospheric Sciences*, **25**, 856–864. (in Chinese with English abstract)

Hagen, M., and S. A. Yuter, 2003: Relations between radar reflectivity, liquid-water content, and rainfall rate during the MAP SOP. *Quart. J. Roy. Meteor. Soc.*, **129**, 477–493.

He, Y., and G. P. Li, 2013: Numerical experiments on influence of Tibetan Plateau on persistent heavy rain in South China. *Chinese Journal of Atmospheric Sciences*, **37**, 933–944. (in Chinese with English abstract)

Hu, Z. J., X. F. Lou, S. W. Bao, and X. B. Wang, 1998: A simplified explicit scheme of phase-mixed cloud and precipitation. *Journal of Applied Meteorological Science*, **9**, 257–264. (in Chinese with English abstract)

Huang, R. H., 1985: The numerical simulation of the three-dimensional teleconnections in the summer circulation over the Northern Hemisphere. *Adv. Atmos. Sci.*, **2**, 81–92, doi: 10.1007/BF03179740.

Huang, R. H., and F. Y. Sun, 1994: Impacts of the thermal state and the convective activities in the tropical western warm pool on the summer climate anomalies in East Asia. *Chinese Journal of Atmospheric Sciences*, **18**, 141–151. (in Chinese with English abstract)

Kong, F. Y., M. Y. Huang, and H. Y. Xu, 1990: Three-dimensional numerical simulation of ice phase microphysics in cumulus clouds, part I: Model establishment and ice phase parameterization. *Scientia Atmospherica Sinica*, **14**, 441–453. (in Chinese with English abstract)

Kozu, T., and K. Nakamura, 1991: Rainfall parameter estimation from dual-radar measurements combining reflectivity profile and path-integrated attenuation. *J. Atmos. Ocean Technol.*, **8**, 259–271.

Li, X., and Z. Su, 2014: Suppression of light precipitation by air pollution: A comparison between observations in South China and the Tibetan Plateau. *Acta Meteorologica Sinica*, **72**, 596–605. (in Chinese with English abstract)

Li, X. S., Y. L. Luo, and Z. Y. Guan, 2014: The persistent severe rainfall over southern China in June 2010: The evolution of synoptic systems and the Tibetan Plateau's heating effect. *Acta Meteorologica Sinica*, **72**, 428–446. (in Chinese with English abstract)

Liao, F., H. Deng, Q. L. Wan, J. X. Qian, H. J. Huang, and W. K. Mao, 2011: Observation studies on characteristics of raindrop size distribution of two typical summer thunderstorm cases in the Pearl River Delta. *Plateau Meteorology*, **30**, 798–808. (in Chinese with English abstract)

Lin, Y. L., R. D. Farley, and H. D. Orville, 1983: Bulk parameterization of the snow field in a cloud model. *J. Climate Appl. Meteor.*, **22**, 1065–1092.

Liu, H. Y., and H. C. Lei, 2006: Characteristics of rain from stratiform versus convective cloud based on the surface raindrop data. *Chinese Journal of Atmospheric Sciences*, **30**, 693–702. (in Chinese with English abstract)

Liu, H. Y., H. B. Chen, H. C. Lei, and Y. X. Wu, 2008: Relationship between rain rate and radar reflectivity based on the raindrop distribution data in Beijing during 2004. *Acta Meteorologica Sinica*, **66**, 125–129. (in Chinese with English abstract)

Liu, L. P., J. M. Feng, R. Z. Chu, Y. J. Zhou, and K. Ueno, 2002: The diurnal variation of precipitation in monsoon season in the Tibetan Plateau. *Adv. Atmos. Sci.*, **19**, 365–378, doi: 10.1007/s00376-002-0028-6.

Liu, L. P., R. Mou, X. Y. Xu, and Z. Q. Hu, 2007: Dynamic and microphysical structures of a squall line system and effects of rain drop size distribution on precipitation. *Acta Meteorologica Sinica*, **65**, 601–611. (in Chinese with English abstract)

Marshall, J. S., and W. M. K. Palmer, 1948: The distribution of raindrops with size. *J. Meteor.*, **5**, 165–166.

Niu, S. J., X. L. An, and J. R. Sang, 2002: Observational research on physical feature of summer rain dropsize distribution under synoptic systems in Ningxia. *Plateau Meteorology*, **21**, 37–44. (in Chinese with English abstract)

Porcùa, F., L. P. D'Adderioa, F. Prodib, andC. Caracciolo, 2014: Rain drop size distribution over the Tibetan Plateau. *Atmospheric Research*, **150**, 21–30.

Qing, Q. T., X. R. Liu, X. H. Li, G. X. Chen, and Y. T. Jin, 1994: Analysis of raindrop spectrum of low vortex of cloud system in Chengdu during the period of April to June of 1990. *Journal of Chengdu Institute of Meteorology*, **9**, 24–29. (in Chinese with English abstract)

Rosenfeld, D., and C. W. Ulbrich, 2003: Cloud microphysical properties, processes, and rainfall estimation opportunities. *Meteor. Monogr.*, **30**, 237–258.

Rutledge, S. A., and P. Hobbs, 1983: The mesoscale and microscale structure and organization of clouds and precipitation in midlatitude cyclones. VIII: A model for the "second-feeder" process in warm-frontal rainbands. *J. Atmos. Sci.*, **40**, 1185–1206.

Shi, A. L., G. G. Zheng, G. Huang, and Y. Q. Zhou, 2004: Characteristics of raindrop spectra of stratiform cloud precipitation in autumn 2002 in Henan Province. *Meteorological Monthly*, **30**, 12–17. (in Chinese with English abstract)

Shi, J. S., W. Zhang, T. Y. Chen, J. R. Bi, and M. He, 2008a: Raindrop-size distribution characteristics of the northern face of Qilian Mountains in the summer of 2006. *Journal of Lanzhou University Sciences (Natural Sciences)*, **44**, 55–61. (in Chinese with English abstract)

Shi, X. Y., X. D. Xu, H. Wang, and D. Y. Qin, 2008b: Characteristics of moisture transport in middle and lower reaches of Yangtze River and its variation trend. *Journal of Hydraulic Engineering*, **39**, 596–603. (in Chinese with English abstract)

Shimizu, S., K. Ueno, H. Fujii, H. Yamada, R. Shirooka, and L. P. Liu, 2001: Mesoscale characteristics and structures of stratiform precipitation on the Tibetan Plateau. *J. Meteor. Soc. Japan*, **79**, 435–461.

Smith, P. L., 2003: Raindrop size distributions: Exponential or gamma-does the difference matter? *J. Appl. Meteor.*, **42**, 1031–1034.

Sun, J., X. F. Lou, Z. J. Hu, and X. S. Shen, 2008: Numerical experiment of the coupling of CAMS complex microphysical scheme and GRAPES model. *Journal of Applied Meteorological Science*, **19**, 315–325. (in Chinese with English abstract)

Tao, S. Y., and Y. H. Ding, 1981: Observational evidence of the influence of the Qinghai-Xizang (Tibet) Plateau on the occurrence of heavy rain and severe convective storms in China. *Bull. Amer. Meteor. Soc.*, **62**, 23–30.

Tokay, A., and D. A. Short, 1996: Evidence from tropical raindrop spectra of the origin of rain from stratiform versus convective clouds. *J. Appl. Meteor.*, **35**, 355–371.

Ueno, K., H. Fujii, H. Yamada, and L. P. Liu, 2001: Weak and frequent monsoon precipitation over the Tibetan Plateau. *J. Meteor. Soc. Japan*, **79**, 419–434.

Uijlenhoet, R., 2001: Raindrop size distributions and radar reflectivity-rain rate relationships for radar hydrology. *Hydrology and Earth System Sciences*, **5**, 615–628.

Ulbrich, C. W., 1983: Natural variations in the analytical form of the raindrop size distribution. *J. Climate Appl. Meteor.*, **22**, 1764–1775.

Ulbrich, C. W., and D. Atlas, 1998: Rainfall microphysics and radar properties: Analysis methods for drop size spectra. *J. Appl. Meteor.*, **37**, 912–923.

Uyeda, H., and Coauthors, 2001: Characteristics of convective clouds observed by a Doppler radar at Naqu on Tibetan Plateau during the GAME-Tibet IOP. *J. Meteor. Soc. Japan*, **79**, 463–474.

Xu, S. Z., G. J. Zhu, Q. Yin, Z. R. Cheng, B. Geng, and Y. M. Zhuang, 1990: The Z-R relationship of precipitation in Wuhan and Yichang areas. *Journal of Nanjing Institute of Meteorology*, **13**, 572–575. (in Chinese with English abstract)

Xu, Y. M., 1992: Radar echo features and their relations to rainfall for heavy frontal rains in the pearl river delta. *Journal of Tropical Meteorology*, **8**, 174–180. (in Chinese with English abstract)

Xue, J. S., S. Y. Zhuang, G. F. Zhu, H. Zhang, Z. Q. Liu, Y. Liu, and Z. R. Zhuang, 2008: Scientific design and preliminary results of three-dimensional variational data assimilation system of GRAPES. *Chinese Science Bulletin*, **53**, 3446–3457.

Zhang, G. Q., A. P. Sun, W. F. ZHOU, L. J. Wang, and H. B. Xiao, 2009: Preliminary study on the character of raindrop spectrum and precipitation mechanism in Menyuan of Qinghai. *Plateau Meteorology*, **28**, 77–84. (in Chinese with English abstract)

Zhang, J. C., and Q. J. Liu, 2006: Analysis of cloud schemes in simulation of short-term climatic process. *Meteorological Monthly*, **32**, 3–12. (in Chinese with English abstract)

Zhao, G., R. Chu, T. Zhang, J. Li, J. Shen, and Z. Wu, 2011: Improving the rainfall rate estimation in the midstream of the Heihe River Basin using raindrop size distribution. *Hydrology and Earth System Sciences*, **15**, 943–951.

Zhuang, W., L. P. Liu, G. L. Wang, and Z. H.Cui, 2013: Radar-derived quantitative precipitation estimation in complex terrain area in Qinghai-Xizang plateau. *Plateau Meteorology*, **32**, 1224–1235. (in Chinese with English abstract)